Journal of Solid State Chemistry **161,** 312–318 (2001)
doi:10.1006/jssc.2001.9317, available online at http://www.idealibrary.com on IDEAL®

Preparation, Crystal Structure, Vibrational Spectra, and Thermal Behavior of *N, N′*-Dimethylpiperazinium(2+) Hydrogen Selenite

Ivan Němec,[1] Vít Chudoba, David Havlíček, Ivana Císařová, and Zdeněk Mička

Department of Inorganic Chemistry, Faculty of Science, Charles University of Prague, Albertov 2030, 128 40 Prague 2, Czech Republic

Received March 6, 2001; in revised form June 21, 2001; accepted July 16, 2001

The X-ray structural analysis of *N,N′*-dimethylpiperazinium(2+) hydrogen selenite has been carried out. The substance crystallizes in the orthorhombic space group *Pbcn*, $a = 14.682(2)$, $b = 6.4910(10)$, $c = 13.065(2)$ Å; $V = 1245.1(3)$ Å^3, $Z = 8$, $R = 0.0234$ for 2135 observed reflections. The cations of trans-*N, N′*-dimethylpiperazinium(2+) in the chair conformation are arranged roughly plane-parallel above one another. Hydrogen selenite anions linked by H-bonds form infinite chains, which are interconnected with *N, N′*-dimethylpiperazinium(2+) groups by N–H ⋯ O hydrogen bonds. The FTIR and FT Raman spectra of natural and deuterated compounds were recorded and interpreted. The FTIR spectra were studied down to a temperature of 90 K. The thermoanalytical properties were studied by the TG, DTG, and DTA methods in the 293–573 K temperature range. DSC measurements were carried out in the 95–403 K temperature range. No thermal effect indicating phase transition was observed in this temperature region. ©2001 Academic Press

Key Words: ***N, N′*-dimethylpiperazinium(2+) hydrogen selenite; crystal structure; vibrational spectra; thermal behavior.**

INTRODUCTION

Many members of the hydrogen selenite family $MH_3(SeO_3)_2$, $MHSeO_3$ and hydrogen selenates $M_4H_2(SeO_4)_3$, $M_4MH_3(SeO_4)_4$, and $MHSeO_4$ types, where M is an alkali metal or ammonium, exhibit interesting physical and structural properties, and much research effort has been devoted to these compounds. However, a minimal amount of attention has been paid in the literature to similar compounds in which the alkali metal ion was substituted by an organic cation. For example, only a few crystal structures of organic nitrogen-containing hydrogen selenites have been published so far (1–5).

This work is part of our project of searching for new hydrogen-bonded materials exhibiting ferroelectric properties or proton conductivity within the group of acidic oxysalts of selenium with organic nitrogen-containing bases.

The title novel compound *N,N′*-dimethylpiperazinium (2 +) hydrogen selenite ($Me_2pipz(HSeO_3)_2$), was prepared and intensively studied. Congruently soluble $Me_2pipz(HSeO_3)_2$ is the only salt formed in the *N,N′*-dimethylpiperazine–selenious acid–water system. From this point of view, comparison with the piperazine–H_2SeO_3–H_2O system is interesting, where two different salts with different anions were isolated (6), piperazinium(2 +) selenite monohydrate and piperazinium(2 +) diselenite.

In addition to determining crystal structure, we measured (and interpreted) the vibrational spectra of polycrystalline $Me_2pipz(HSeO_3)_2$ and of its deuterated analogue. FTIR measurements down to low temperatures (90 K) and DSC measurements in a broad temperature interval were carried out to elucidate the existence of possible phase transitions.

EXPERIMENTAL

Crystals of $Me_2pipz(HSeO_3)_2$ were prepared by slow spontaneous evaporation of a solution of *N,N′*-dimethylpiperazine (98%, Aldrich) and selenious oxide (99.8%, Aldrich) (in a molar ratio of 1:2) at laboratory temperature. The colorless crystals obtained were collected under vacuum on an S2 frit, washed with a small amount of cold water and ethanol, and dried in the air. The selenium content was determined iodometrically (7) (theoretical content 42.4%, found 42.0%). Elemental analysis results for C, H, and N (19.5% C, 4.8% H, 7.4% N) agree well with theoretical content (19.4% C, 4.9% H, 7.5% N).

The N,O-deuterated compound $(CH_2)_4(ND^+CH_3)_2\cdot(DSeO_3^-)_2$ was prepared similarly as a natural compound using D_2O (99%) as a solvent, and the product was crystallized in a desiccator over KOH.

The X-ray data collection for the $Me_2pipz(HSeO_3)_2$ single crystal was carried out on an Enraf–Nonius CAD4-MACH III four-circle diffractometer (Mo$K\alpha$ radiation,

---

[1] To whom correspondence should be addressed. E-mail: agnemec@natur.cuni.cz.

0022-4596/01 $35.00

graphite monochromator). The temperature of the crystal was controlled by an Oxford Cryosystems liquid nitrogen Cryostream Cooler. Intensities of diffractions were corrected for the Lorentz-polarization effects and for absorption. The positions of the nonhydrogen atoms were determined using direct methods (SIR-92 (8)), and the hydrogen atoms were localized on differential Fourier maps. The thermal parameters for the nonhydrogen atoms were refined anisotropically and, for the hydrogen atoms, isotropically. Refine-

TABLE 1
Basic Crystallographic Data, Data Collection, and Refinement Parameters of $Me_2pipz(HSeO_3)_2$

Empirical formula	$C_6H_{18}N_2O_6Se_2$	X-ray powder diffraction method
Formula weight	372.14	
Temperature	150.0(1) K	298 K
Wavelength	0.71069 Å	1.54178 Å
Crystal system, space group	orthorhombic, *Pbcn*	
Unit cell dimensions	$a = 14.682(2)$ Å $b = 6.4910(10)$ Å $c = 13.065(2)$ Å	$a = 14.691(4)$ Å $b = 6.492(2)$ Å $c = 13.054(4)$ Å
Volume	$V = 1245.1(3)$ Å^3	$V = 1244.9(6)$ Å^3
Z, Calculated density	8, 1.985 g.cm^{-3}	
Absorption coefficient	5.954 mm^{-1}	
F(000)	736	
Crystal size	0.5 × 0.35 × 0.25 mm	
Theta range for data collection	2.77 to 24.98°	
Range of *h*, *k* and *l*	$-17 \rightarrow 17$, $0 \rightarrow 7$, $0 \rightarrow 15$	
Reflections collected/unique (R_{int})	2135/1095 (0.0537)	
Refinement method	Full-matrix least-squares on F^2	
Data/restraints/parameters	1095/0/110	
Absorption correction	empirical	
T_{min}	0.620	
T_{max}	0.990	
Goodness-of-fit on F^2	1.170	
Final *R* indices [$I > 2\sigma(I)$]	R1 = 0.0234, wR2 = 0.0605	
R indices (all data)	R1 = 0.0309, wR2 = 0.0630	
Extinction coefficient	0.049(2)	
Largest diff. max. and min.	0.371, −1.017 e.Å^{-3}	
No. and Θ range of reflections for unit cell determination	25, 13–14°	
Scan technique	Θ–2Θ	
No. of standard reflections	3	
Standard reflections monitored in interval	60 min.	
Intensity variation	2.5%	
Function minimized	$[\sum(w(F_o^2 - F_c^2))^2/\sum(w(F_o^2)^2]^{1/2}$	
Weighting scheme	$w = [\sigma^2(F_o^2) + (0.0296P)^2 + 0.00P]^{-1}$ $P = [F_o^2 + 2F_c^2]/3$	

TABLE 2
Fractional Atomic Coordinates (for Non-H Atoms×10^4, for H Atoms×10^3) and Equivalent (×10^4) or Isotropic(×10^3) Displacement Factors with Standard Deviations in Brackets for $Me_2pipz(HSeO_3)_2$ $U_{eq} = 1/3\sum_i\sum_j U_{ij}a_i^*a_j^*\mathbf{a}_i\mathbf{a}_j$

	x	*y*	*z*	U_{eq} (Å^2)
Se1	3755(1)	4026(1)	2328(1)	16(1)
O1	2874(1)	4916(3)	1517(1)	30(1)
O2	3390(2)	1686(3)	2618(2)	32(1)
O3	4531(1)	3695(2)	1415(1)	21(1)
C1	4932(2)	1486(4)	−807(2)	18(1)
C2	4170(2)	−1002(3)	307(2)	17(1)
C3	3280(2)	1741(4)	−535(2)	21(1)
N1	4165(2)	1174(3)	−74(2)	15(1)
H1	246(3)	551(6)	184(3)	52(11)
H10	422(2)	190(4)	48(2)	16(7)
H11	491(2)	285(5)	−100(2)	28(7)
H12	481(2)	53(4)	−141(2)	9(6)
H21	362(2)	−119(4)	71(3)	34(10)
H22	404(2)	−182(3)	−30(2)	7(5)
H31	326(2)	312(5)	−68(2)	30(8)
H32	279(2)	143(3)	−6(2)	25(7)
H33	317(2)	94(4)	−113(3)	26(8)

TABLE 3
Bond Lengths (Å) and Selected Angles (°) for $Me_2pipz(HSeO_3)_2$

Se1–O1	1.769(2)	C1–N1–C2	109.7(2)
Se1–O2	1.654(2)	C1–N1–C3	111.6(2)
Se1–O3	1.664(2)	C2–N1–C3	112.0(2)
C1–N1	1.491(3)	N1–C1–H11	107(2)
C1–C2^i	1.505(4)	N1–C1–H12	106(2)
C1–H11	0.92(3)	H11–C1–H12	111(2)
C1–H12	1.02(3)	C2^i–C1–H11	110(2)
C2–N1	1.497(3)	C2^i–C1–H12	112(1)
C2–H21	0.97(3)	N1–C2–H21	107(2)
C2–H22	0.98(2)	N1–C2–H22	104(1)
C3–N1	1.479(3)	H21–C2–H22	102(2)
C3–H31	0.92(3)	C1^i–C2–H21	118(2)
C3–H32	0.98(3)	C1^i–C2–H22	114(1)
C3–H33	0.95(3)	N1–C3–H31	111(2)
		N1–C3–H32	110(2)
		N1–C3–H33	110(2)
O1–Se1–O2	101.6(1)	H31–C3–H32	108(2)
O1–Se1–O3	96.5(1)	H31–C3–H33	111(2)
O2–Se1–O3	105.5(1)	H32–C3–H33	107(2)
Se1–O1–H1	112(3)	C1–N1–H10	113(2)
N1–C1–C2^i	110.7(2)	C2–N1–H10	104(2)
N1–C2–C1^i	110.2(2)	C3–N1–H10	107(2)

Hydrogen bonds:

Donor–H	Donor … Acceptor	H … Acceptor	Donor–H … Acceptor
O1–H1	O1 … O2^{ii}	H1 … O2^{ii}	O1–H1 … O2^{ii}
0.84(4)	2.615(3)	1.78(4)	176(4)
N1–H10	N1 … O3	H10 … O3	N1–H10 … O3
0.87(3)	2.598(3)	1.75(3)	166(3)

Note. Equivalent positions: (i) $-x+1$, $-y$, $-z$; (ii) $-x+\frac{1}{2}$, $y+\frac{1}{2}$, z.

ment of the coordinates and the thermal parameters was carried out by the least squares method using the SHELXL-97 program (9). The basic crystallographic data and the details of the measurement and refinement are summarized in Table 1. A list of the observed and calculated structural factors and the anisotropic displacement factors are available from the authors upon request.

The lattice parameters were refined at laboratory temperature using the X-ray powder diffraction method. The measurement was carried out on a Freiberg (Germany) URD 6 instrument (Cu*Kα* radiation; Ni filter without a monochromator; range of 10–100° 2*θ*; step 0.02°; 10 s per step). The results were processed by the ZDS set of programs (10).

The infrared spectra of nujol and fluorolube mulls were recorded on a Mattson Genesis FTIR spectrometer (2-cm^{-1} resolution; Beer–Norton medium apodization) in the 400–4000 cm^{-1} region. Low-temperature measurements were carried out by the nujol mull method in a low-temperature cell with KBr windows in the 298–90 K interval. The temperature was controlled by a Fe-Const. thermocouple. The analog signal was processed on a PC using the AX5232 temperature measurement board.

FAR IR spectra of nujol mull (PE windows) were recorded on a Nicolet Magna 760 FTIR spectrometer (Solid Substrate beamsplitter; DTGS on PE detector; 4-cm^{-1} resolution, Happ–Genzel appodization) in the 50–600 cm^{-1} region.

The Raman spectra of polycrystalline samples were recorded on a Bruker Equinox 55/S FTIR spectrometer with a FRA 106/S Raman module (2-cm^{-1} resolution, Blackman–Harris 4-Term apodization; 1064 nm NdYAG laser excitation; 250 mW power at the sample) in the 50–4000 cm^{-1} region.

The DSC measurements were carried out on a Perkin–Elmer DSC 7 power-compensated apparatus in the 95–403 K temperature region (helium or nitrogen atmosphere). A heating rate of 10 K/min was selected to measure approximately 10 mg of finely ground sample placed in aluminum capsule.

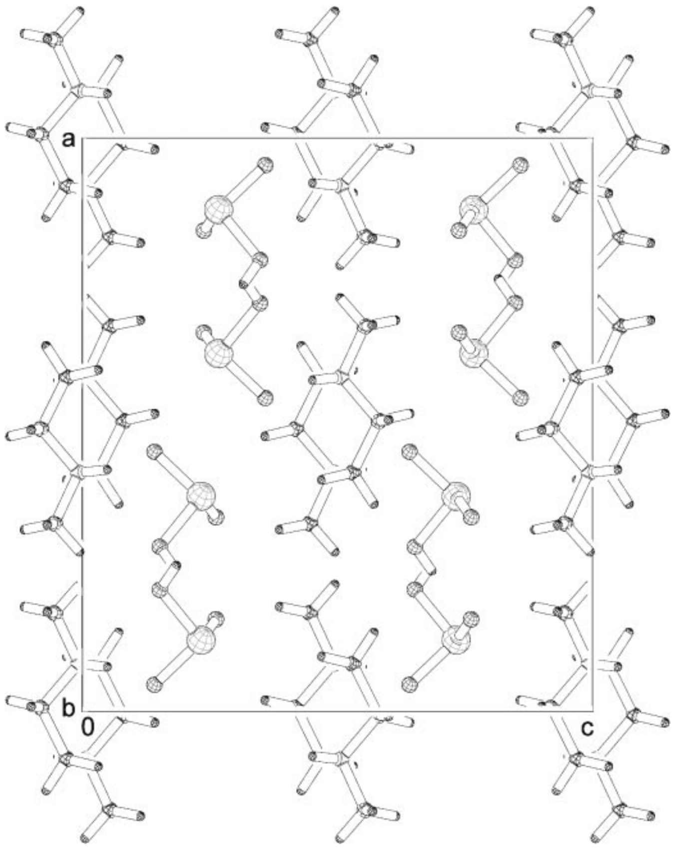

FIG. 2. Packing scheme of $Me_2pipz(HSeO_3)_2$ (projection to *xz* plane). Dashed lines indicate hydrogen bonds.

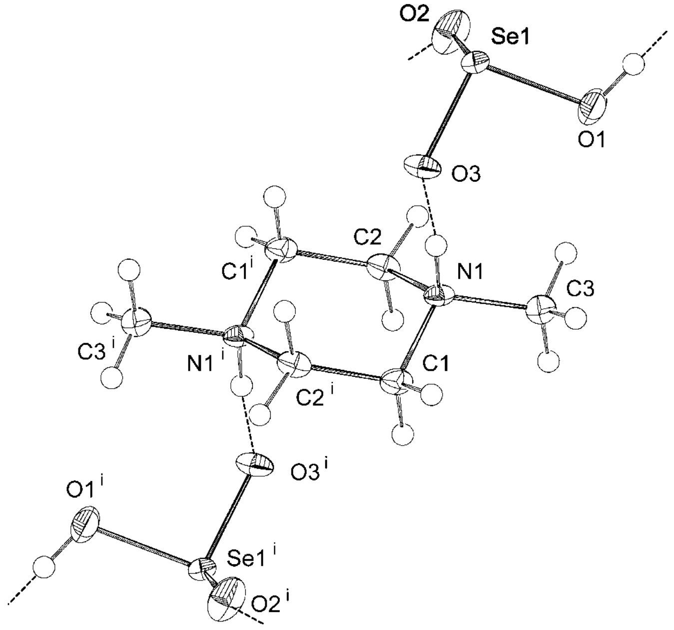

FIG. 1. Atom numbering of $Me_2pipz(HSeO_3)_2$. Dashed lines indicate hydrogen bonds.

TABLE 4
The Results of the Nuclear Site Group Analysis for $Me_2pipz(HSeO_3)_2$

D_{2h}^{14}		A_g	A_u	B_{1g}	B_{1u}	B_{2g}	B_{2u}	B_{3g}	B_{3u}
	Acoustical				1		1		1
External modes	Translational	3	6	3	5	3	5	3	5
	Librational	6	3	6	3	6	3	6	3
Internal modes		42	42	42	42	42	42	42	42
	Total	51	51	51	51	51	51	51	51
Activity	IR				*z*		*y*		*x*
	Raman	α_{xx}, α_{yy}, α_{zz}		α_{xy}		α_{xz}		α_{yz}	

TABLE 5
Correlation Analysis of $HSeO_3^-$ Internal Modes in $Me_2pipz(HSeO_3)_2$ Crystal

Free ion modes[a]	Degrees of freedom	Free ion symmetry C_s	Site symmetry C_1	Factor group symmetry D_{2h}	Vibrational modes	Activity IR	Activity Raman
ν_1 ν Se–O(H)	8	A'		A_g	ν_1–ν_6		α_{xx}, α_{yy}, α_{zz}
ν_2 ν_s Se–O	8			A_u	ν_1–ν_6		
ν_3 δ_s O–Se–O(H)	8			B_{1g}	ν_1–ν_6		α_{xy}
ν_4 δ O–Se–O	8		A	B_{1u}	ν_1–ν_6	z	
				B_{2g}	ν_1–ν_6		α_{xz}
ν_5 ν_{as} Se–O	8	A''		B_{2u}	ν_1–ν_6	y	
ν_6 δ_{as} O–Se–O(H)	8			B_{3g}	ν_1–ν_6		α_{yz}
				B_{3u}	ν_1–ν_6	x	

[a] The OH group was assumed to be a single atom.

The thermoanalytical properties were studied using TG, DTG, and DTA recordings. The measurements were carried out on a Derivatograph OD-102 instrument (MOM Budapest). A static atmosphere (air) was used in a temperature range of 293–573 K and at a heat rate of 10 K/min.

RESULTS AND DISCUSSION

Crystal Structure

The fractional atomic coordinates of $Me_2pipz(HSeO_3)_2$ are given in Table 2. Bond lengths and angles including those for the hydrogen bonds are listed in Table 3. The atom numbering can be seen in Fig. 1, and the packing scheme is depicted in Fig. 2 (PLATON software (Ref. 11)).

The crystal structure of $Me_2pipz(HSeO_3)_2$ consists of the *N,N′*-dimethylpiperazinium(2 +) and $HSeO_3^-$ ions, which are mutually connected by a system of hydrogen bonds. The cations of trans-*N,N′*-dimethylpiperazinium(2 +) in the chair conformation are arranged roughly plane-parallel above one another. A similar cation arrangement was also observed for the related salts of piperazine and selenic acid (12) or selenious acid (6). In contrast, the trans-*N,N*'-

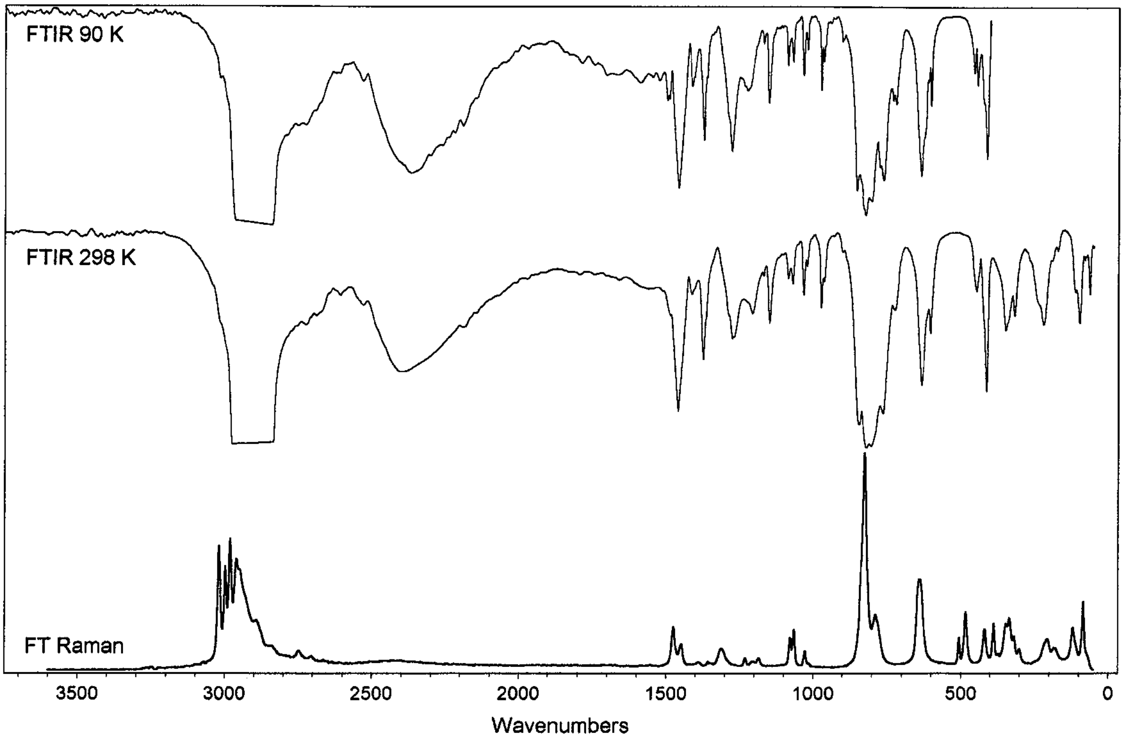

FIG. 3. FTIR (nujol mull) and FT Raman spectra of $Me_2pipz(HSeO_3)_2$.

TABLE 6
FTIR and FT Raman Spectra of Me$_2$pipz(HSeO$_3$)$_2$

Assignment	IR 298 K	IR 90 K	Raman (peak intensity)	Assignment	IR 298 K	IR 90 K	Raman (peak intensity)
νCH$_3$, νCH$_2$	3020m	3018m	3020(58)‡	νC–C, νC–N, δ–N–C–H			1078(16)
	2997m	n.o.[a]	2999(49)	γN–H...O	1072w	1072w	
	2979m	n.o.[a]	2982(62)	νC–C, νC–N, – δN–C–H			1065(19)
	2960m	n.o.[a]	2960(51)	δNCH, δCCH, νCN	1034m	1036m	1028(9)
			2949(46)	γO–H...O	1022w	1023w	
?	2930mb	n.o.[a]	2892(22)	δNCH, δCCH, νCN			1016(3)
			2843(11)	δN–C–H, δC–C–H	974m	975m	
νO–H $\cdots$ O	2770mb	n.o.[a]	2747(9)		965sh	967w	
			2705(6)	?	903w	904w	
νN–H $\cdots$ O	2390mb	2365sb	2420(5)	ν_sSe–O (ν_2 HSeO$_3^-$)	844s	855s	838sh
		2195m		ν_sSeO (ν_2 HSeO$_3^-$), νCN	821s	824s	826(100)
?	1800mb	1790w		ν_{as}Se–O (ν_5 HSeO$_3^-$)	805s	804s	788(25)
		1745w				776s	781(22)
	1700mb	1705m			764s	763s	
		1665m				732m	
?		1590m		νSe–OH (ν_1 HSeO$_3^-$)	634s	637s	642(41)
δNH$^+$	1544mb	1550m				625sh	638(41)
		1526m				612m	
		1500m			604m	604m	
	1496m	1492m		δC–N–C, δN–C–C			505(16)
δ_{as}CH$_3$, δCH$_2$	1470m	n.o.[a]	1476(20)	δO–Se–O (ν_4 HSeO$_3^-$),		457m	483(27)
	1456m	n.o.[a]	1449(12)	δC–N–C	448m	446m	
δ_sCH$_3$, twiCH$_2$	1415m	1415m		δO–Se–O (ν_4 HSeO$_3^-$)		425sh	420(19)
	1405sh	1408sh	1390(4)		414s	413s	
	1371m	n.o.[a]		δC–N–C, δN–C–C			388(22)
δN–C–H, δC–C–H			1357(4)	δ_{as}HO–Se–O (ν_6 HSeO$_3^-$)	349m		346(21)
			1345(3)		338sh		334(24)
			1311(10)	δ_sHO–Se–O (ν_3 HSeO$_3^-$)	318m		319(16)
δSe–O–H, δCNH,	1290sh	1290sh					302(10)
δNCH, δCCH	1275m	1279m		?	240sh		
		1225m	1231(6)	τCH$_3$	220m		206(14)
δC–C–H, δN–C–H	1209m		1204(4)		190w		181(10)
			1184(6)		171w		
νC–N, δC–C–H	1171w	1171w		External modes	112m		120(13)
	1150m	1154m			98m		85(33)
γN–H $\cdots$ O	1087w	1089w			64m		

Note. Abbreviations: s, strong; m, medium; w, weak; b, broad; sh, shoulder; ν, stretching; δ, deformation or in–plane bending; γ, out–of–plane bending; twi, twisting; τ, torsional; $_s$, symmetric; $_{as}$, asymmetric.

[a] not observed due to nujol bands.

dimethylpiperazinium(2+) cations have almost perpendicular mutual orientation in the crystal structure of *N*,*N*′-dimethylpiperazinium(2+) selenate dihydrate (12).

However, hydrogen selenite anions linked by intermediate O–H $\cdots$ O hydrogen bonds with a length of 2.62 Å that forming infinite chains along the *b*-axis, by far predominate as the crystal structure forming motif. These chains are interconnected with cations by short (2.60 Å) O $\cdots$ H–N hydrogen bonds, which are the shortest cation–anion H-bonds found in the family of relative compounds of piperazine and its N-methyl derivatives with selenium oxyacids (6, 12). The presence of hydrogen selenite anions in the crystal structure is also confirmed by a corresponding increase of the Se–O(H) bond length (1.769 Å) compared to the Se–O bond lengths (1.654 and 1.664 Å). Slight differences in the Se–O bond lengths can be correlated very well with the different participation of O2 and O3 atoms in the hydrogen bonds of O $\cdots$ H–O and O $\cdots$ H–N types (see Table 3).

Analysis of the Vibrational Spectra

The number of normal modes of the crystals was determined by nuclear site group analysis (13). Standard correlation methods (14) were used for more detailed study of the

TABLE 7
FTIR Spectra of N,O–deuterated $Me_2pipz(DSeO_3)_2$

Assignment	(cm^{-1})	Assignment	(cm^{-1})
νCH_3, νCH_2	3021m	δC–N–H, δN–C–H, δC–C–H	1272m
	2998m		1215m
	2981m	νC–N, δC–C–H, $\delta N\text{–}D^+$	1150m
	2960m		1143m
?	2893w	δN–C–H, δC–C–H, νC–N	1048m
	2801w	δN–C–H, δC–C–H, δSe–O–D	997w
	2726w		981m
νO–D $\cdots$ O	2070mb		959w
νN–D $\cdots$ O	1800m	δSe–O–D	927m
	1760m	ν_sSe–O (ν_2 $DSeO_3^-$)	835s
	1685m	ν_sSe–O (ν_2 $DSeO_3^-$), νC–N	822s
	1650m	γO–D...O	722w
	1580m	ν_{as}Se–O (ν_5 $DSeO_3^-$)	796s
$\delta_{as}CH_3$, δCH_2	1470m		769s
	1459m	νSe–OD (ν_1 $DSeO_3^-$)	624s
	1452m		601m
$\delta_s CH_3$, twiCH_2	1415m	δO–Se–O (ν_4 $DSeO_3^-$)	445m
	1373m		416s
	1311w		

expected vibrational features of hydrogen selenite groups. The results obtained are presented in Tables 4 and 5. Orthorhombic $Me_2pipz(HSeO_3)_2$ crystals belong in the *Pbcn* (D_{2h}^{14}) space group with 17 atoms per asymmetric unit ($Z = 8$). All the atoms occupy eightfold positions $d(C_1)$. Two types of species present in the unit cell, *N*,*N*′-dimethylpiperazinium(2 +) cation and $HSeO_3^-$ anion, occupying fourfold positions $a(C_i)$ and eightfold positions $d(C_1)$, respectively, were considered in more detailed calculations of the internal and external modes. However, the expected level of factor group splitting has not been observed even in low-temperature IR spectra. This fact could be explained by small interion interaction in the unit cell and also in terms of the fact that all the measurements were carried out on polycrystalline samples.

Vibrational Spectra

The vibrational spectra of $Me_2pipz(HSeO_3)_2$ are depicted in Fig. 3, and the wavenumbers of the maxima are given in Tables 6 and 7. The assignment of vibrational bands is based on previous spectroscopic study of *N*,*N*′-dimethylpiperazine (15–17) and is also consistent with the results obtained for the similar compound with selenic acid (12). The IR spectra of N,O-deuterated compound were measured to confirm this interpretation.

The observed positions of broad medium-intensity bands of O–H and N–H stretching vibrations correspond well (according to (18, 19)) to hydrogen bonds lengths found in the crystal structure (2.62 and 2.60 Å of O–H $\cdots$ O and N–H $\cdots$ O, respectively). Corresponding shifts of all the bands discussed occur in the spectra of the deuterated compound. The weak bands in the IR spectrum in the region 1090–1020 cm^{-1} which are sensitive to deuteration can be assigned to out-of-plane O–H $\cdots$ O and N–H $\cdots$ O bending vibrations.

The sharp bands in the 3020–2950 cm^{-1} region are characteristic for the stretching vibrations of the CH_2 and CH_3 groups. Manifestations of deformation vibrations of these groups are localized in the 1470–1370 cm^{-1} region.

The existence of *N*,*N*′-dimethylpiperazinium(2 +) cations in the crystal structue is also reflected in the bands of the δNH^+ deformation vibrations in the infrared spectrum of 1550–1490 cm^{-1}. Their more complex structure (especially in the low-temperature spectrum) is apparently caused by interaction with overtones or combination modes. The expected shift of these bands to lower wavenumbers occurs in the spectrum of the deuterated analogue.

Multiple bands of the deformation vibrations of the dimethylpiperazine skeleton can be observed below cca. 1360 cm^{-1} in the both IR and Raman spectra.

The clear indications of the presence of $HSeO_3^-$ anion in the crystal structure are, beside the Se–O valence vibrations position, broader bands of δSe–O–H vibrations at 1290–1275 cm^{-1}. These bands, which are complicated by overlapping with the mixed vibration δCNH, δNCH, δCCH, are sensitive to deuteration, as expected.

Manifestations of external modes were recorded in the Raman and FAR IR spectra in the region below 150 cm^{-1}.

Thermal Behavior

$Me_2pipz(HSeO_3)_2$ is stable in the air up to 368 K, where it start to lose water of composition. This process is complete at ca. 403 K, where further decomposition begins.

Compounds were further studied by the DSC method in the temperature interval 95–365 K. No thermal effect was observed in the entire interval.

The FTIR spectra (in mid-infrared region) were recorded in the temperature interval from 298 to 90 K. No changes that would indicate the occurrence of structural phase transition were observed during decrease in the temperature of the sample. The minor differences found in the low-temperature spectrum (i.e., narrowing and partial separation of the vibrational bands) are a result of the temperature effect.

As the space group of $Me_2pipz(HSeO_3)_2$ is centrosymmetric (*Pbcn*) and any phase transition to a polar phase was not observed, the existence of significant dielectric properties (specifically ferroelectric) can be completely excluded. Analogously, the absence of any phase transitions at elevated temperature excludes the formation of phases with contingent proton conductivity.

ACKNOWLEDGMENTS

This study was carried out with the financial assistance of the Grant Agency of the Czech Republic, Grant 203/98/1198, and the Grant Agency of Charles University of Prague, Grant 13/1998/B CH, and is a part of the long-time Research Plan of the Faculty of Science "Structure, Dynamics and Function of Molecular and Supramolecular Assemblies" (MSM11310001).

REFERENCES

1. W. Krumbe and S. Haussuhl, *Z. Kristallogr.* **179,** 132 (1987).
2. J. A. Paixão, A. Matos Beja, M. Ramos Silva, and M. Martín-Gil, *Acta Crystallogr. Sect. C, Cryst. Struct. Commun.* **53**(8), 1113 (1997).
3. I. Němec, I. Císařová, and Z. Mička, *J. Solid State Chem.* **140,** 71 (1998).
4. E. de Matos Gomes, A. Matos Beja, J. A. Paixão, L. Alte de Veiga, M. Ramos Silva, J. Martín-Gil, and F. J. Martín-Gil, *Z. Kristallogr.* **210,** 929 (1995).
5. J. A. Paixão, A. Matos Beja, M. Ramos Silva, and M. Martín-Gil, *Z. Krystallogr. – New Cryst. Struct.* **212**(1), 51 (1997).
6. D. Havlíček, V. Chudoba, I. Němec, I. Císařová, and Z. Mička, *J. Mol. Struct.*, in print.
7. M. Zh. Ganitskij and V. I. Zelinokrajte, *Zh. Neorg. Chim.* **2,** 1341 (1957).
8. A. Altomare, M. C. Burla, M. Camalli, G. Cascarano, C. Giacovazzo, A. Guagliardi, and G. Polidori, *J. Appl. Cryst.* **27,** 435 (1994)
9. G. M. Sheldrick, "SHELXL-97." University of Göttingen, 1997.
10. P. Ondruš, "ZDS 5.14 - Software for Analysis of X-Ray Powder Diffraction Data," 1992.
11. A. L. Spek, *Acta Crystallogr. Sect. A* **46,** C-34 (1990).
12. D. Havlíček, J. Plocek, I. Němec, R. Gyepes, and Z. Mička, *J. Solid State Chem.* **150**(2), 305 (2000).
13. D. L. Rousseau, R. P. Bauman, and S. P. S. Porto, *J. Raman Spectrosc.* **10,** 253 (1981).
14. W. G. Fateley, N. T. McDevit, and F. F. Bentley, *Appl. Spectrosc.* **25,** 155 (1971).
15. N. N. Rubanyuk, S. M. Kim, Kh. Kh. Muldagaliev, and O. V. Agashkin, *Izv. Akad. Nauk. Kaz. SSR, Ser. Khim.* **5,** 38 (1986).
16. S. M. Kim, Kh. Kh. Muldagaliev, and O. V. Agashkin, *Izv. Akad. Nauk. Kaz. SSR, Ser. Khim.* **4,** 14 (1989).
17. K. Fukushima, *Bull. Chem. Soc. Jpn.* **52**(10), 2871 (1979).
18. A. Novak, *Struct. Bond.* **18,** 177 (1974).
19. A. Lautie, F. Froment, and A. Novak, *Spectrosc. Lett.* **9**(5), 289 (1976).